

# REGULARIZED SELECTION: A NEW PARADIGM FOR INVERSE BASED REGULARIZED IMAGE RECONSTRUCTION TECHNIQUES

Florentin Kucharczak<sup>12</sup>, Cyril Mory<sup>23</sup>, Olivier Strauss<sup>2</sup>, Frederic Comby<sup>2</sup>, Denis Mariano-Goulart<sup>4</sup>

<sup>1</sup>Siemens Healthineers

<sup>2</sup>LIRMM, Montpellier University/ CNRS, France

<sup>3</sup>Creatis, Univ. Lyon/ UMR 5220, France

<sup>4</sup>CHRU Lapeyronie, Montpellier University, France

## ABSTRACT

In this paper, we present a new regularization paradigm for inverse based regularized image reconstruction techniques. These methods usually attempt to minimize a cost function expressed as the sum of a data-fitting term and a regularization term. The trade-off between both terms is determined by a weighting parameter that has to be set by the user since this trade-off is data dependent. In the approach we present here, we first concentrate on finding a set of eligible candidates for the data fitting term minimization and then select the most appropriate candidate according to the regularization criterion. The main advantage of this method is that it does not require any weighting parameter, and guarantees that no over-regularization can occur. We illustrate this method with a super-resolution reconstruction technique to show its efficiency compared to other competitive methods. Comparisons are carried out with simulated and real data.

**Index Terms**— Regularization, inverse problems, interval-based methods, imprecise modeling, super-resolution.

## 1. INTRODUCTION

In the traditional approach, inverse based regularized reconstruction techniques consist in minimizing a criterion  $\epsilon$  of the form:

$$\epsilon(\mathbf{X}) = \epsilon_1(\mathbf{H}(\mathbf{X}, \mathbf{Y})) + \beta \cdot \epsilon_2(\mathbf{X}), \quad (1)$$

that gathers a data-fitting term  $\epsilon_1$ , that expresses how the output image  $\mathbf{X}$  is linked to the input measurements  $\mathbf{Y}$  via the observation model  $\mathbf{H}$ , and a regularization term  $\epsilon_2$  that aims at discarding inappropriate solutions, preventing over-fitting. Those two terms have to be balanced thanks to a parameter  $\beta$  used to control the regularization level of the solution. Once both  $\epsilon_1$  and  $\epsilon_2$  criteria are chosen (usually expressed as a norm of the output error for  $\epsilon_1$  and of a sparsifying transform of the reconstructed image for  $\epsilon_2$ ), the most challenging problem is to choose the parameter  $\beta$ . Even if some methods present a way to find a suitable value of  $\beta$  [1], this choice remains difficult and fully dependent on the image content. Thus many authors still prefer to regularize the solution by an early stop of an un-regularized reconstruction process [2,3] or to achieve

a post-regularization (i.e. a smoothing of the obtained image) rather than minimizing a regularized criterion. All these methods have in common that setting their regularization parameter ( $\beta$  or iteration number) is difficult and image content dependent.

In this paper, we propose an innovative solution to the problem of balancing data-fitting and regularization, which we call "regularized selection". We propose to first select a convex set of images that fully satisfy the first criterion  $\epsilon_1$ , and then to select, in this convex set, the image that minimizes the regularization criterion  $\epsilon_2$ .

This method is based on previous works that consider more deeply the fitting term  $\mathbf{H}$ . In fact, digital signal-image processing usually relies on an underlying real-valued continuous model, while the processing is achieved by an algorithm working in the digital space, i.e. an integer-valued discrete space. This kind of methods make extensive use of kernels to ensure the interplay between continuous and discrete space. The choice of a particular kernel (e.g. bicubic) can have a major effect especially in inverse based image processing reconstruction techniques. In the last decade, a new generic approach has been proposed in the literature to lower the impact of the discrete-to-continuous interplay modeling in image processing (e.g. [4] in tomography, [5] in image upsampling, [6] in low-pass filtering or [7] in super resolution reconstruction). This approach mainly consists in modeling scant knowledge of the appropriate discrete to continuous interplay by using a non-additive neighborhood function [8] that models a convex set of conventional methods. Due to this modeling, the resulting image is interval-valued, i.e. each pixel value is a real interval. After convergence, this interval-valued image represents the convex set of images that satisfy the first criterion. Until now, the center image has been used to gather the information of the interval-valued image, since this center image is the closest, in the sense of the Haussdorff distance, to the obtained interval valued image. However, the central image being rather noisy when the reconstruction process is carried out till convergence, the reconstruction had to be early stopped to ensure a kind of regularization.

In this paper, we present a method that uses the interval-based modeling of inverse problems to introduce a new reg-

ularization paradigm: the regularized selection. This method has two advantages: it does not require an early stop of the un-regularized interval-valued reconstruction anymore, and the regularized image is protected from over-smoothing by the interval constraint. We illustrate the performance of this approach by applying this new regularized selection method to the super-resolution (SR) technique proposed in [8] and comparing it to other competitive and regularized SR methods. Naturally, such a regularization can be used for any of the above mentioned interval-valued inverse based approaches [4–7].

## 2. INTERVAL-VALUED IMAGE PROCESSING TECHNIQUES

Most inverse based image reconstruction approaches rely on a model of the form:

$$\mathbf{Y} = \mathbf{F}(\mathbf{X}, \kappa, \eta), \quad (2)$$

linking the observations  $\mathbf{Y}$  to the image to be reconstructed  $\mathbf{X}$  via two kernels:  $\kappa$ , the interpolation kernel and  $\eta$ , the PSF of the sensor. The reconstruction of  $\mathbf{X}$  consists in minimizing  $\epsilon$  as defined in (1) with  $\mathbf{H}(\mathbf{X}, \mathbf{Y}) = \mathbf{Y} - \mathbf{F}(\mathbf{X}, \kappa, \eta)$ . In this framework, the role of  $\kappa$  is to ensure the interplay between the discrete domain  $\Omega$ , where measurements and image to be reconstructed are defined, and the continuous domain, where the fitting problem is defined.  $\eta$  is the point spread function (PSF) of the measuring device. For example, in SR problems,  $\kappa$  is an interpolation kernel used to align the low resolution images on the high resolution image to be reconstructed, while  $\eta$  is the PSF of the imager.

Interval-valued inverse based reconstruction techniques consist in replacing at least one of the two kernels ( $\kappa$  or  $\eta$ ) by a maxitive kernel [9]. This replacement allows to represent the fact that the model is imprecisely known, since a maxitive kernel represents a convex family of usual kernels. For example, in [8], a maxitive kernel  $\pi$  has to be chosen to define a convex set  $\mathcal{M}(\pi)$  of the possible PSF of the imager, while the bilinear kernel  $\kappa$  ensures the interpolation. Note that trying to regularize an interval-valued process like a precise one would not be relevant because regularization would apply on the bounds of the reconstructed intervals, which makes no sense according to the modeling we present here. This is the reason why every interval-valued image processing techniques presented in the literature [4–7] consider  $\beta = 0$ . The imprecise model is thus of the form:

$$\underline{\mathbf{Y}} = [\mathbf{Y}, \bar{\mathbf{Y}}] = \underline{\mathbf{F}}(\mathbf{X}, \kappa, \pi), \quad (3)$$

where  $\mathbf{X}$  is the image to be reconstructed and  $\mathbf{Y}$  the set of all the images that would have been obtained by using expression (2) with  $\eta \in \mathcal{M}(\pi)$ . When  $\epsilon_1$  is chosen to be the  $L_2$  norm, then the reconstruction process can be ensured by using the extension of the Schulz iterative algorithm proposed in [10]. Inverting expression (3) consists in starting from a precise observation  $\mathbf{Y}$ , estimating the convex set  $\underline{\mathbf{X}}$  of reconstructed images

that minimizes  $\epsilon_1(\mathbf{Y} - \mathbf{F}(\mathbf{X}, \kappa, \eta))$  with  $\eta \in \mathcal{M}(\pi)$ . In [8], this solution has been proposed to solve an SR interval-valued inverse problem, leading to reconstruct an interval-valued high resolution HR image  $\underline{\mathbf{X}}$ .

## 3. REGULARIZED SELECTION FOR INTERVAL-VALUED IMAGES

The regularized selection techniques consists in considering the reconstructed interval-valued image  $\underline{\mathbf{X}}$  (representing the convex-set of admissible images) to select the most appropriate candidate according to the chosen regularization criterion  $\epsilon_2$ . The selection uses the widely used primal-dual algorithm presented by Chambolle and Pock in [11].

### 3.1. Chambolle-Pock algorithm

The Chambolle-Pock algorithm is an efficient and robust method to solve a problem of the form:

$$\min_{\mathbf{X} \in \mathbb{R}^N} F(A.\mathbf{X}) + G(\mathbf{X}). \quad (4)$$

with  $A$  being a linear operator, and  $F$  and  $G$  being two proper, convex, lower-semi-continuous (l.s.c) functions.

To be as simple and as straightforward as possible, let us use the proximal [12] formulation of the primal-dual algorithm. Its general form is:

$$\begin{cases} v^{(k+1)} = \text{prox}_{\nu F^*}(v^{(k)} + \nu A w^{(k)}) \\ u^{(k+1)} = \text{prox}_{\mu G}(u^{(k)} + \mu A^* v^{(k+1)}) \\ w^{(k+1)} = u^{(k+1)} + \theta(u^{(k+1)} - u^{(k)}), \end{cases} \quad (5)$$

with  $\text{prox}_F(\mathbf{X}) = \underset{\mathbf{Y}}{\text{argmin}} (F(\mathbf{Y}) + \frac{1}{2}|\mathbf{X} - \mathbf{Y}|_2^2)$ ,  $|\bullet|_2$  being the  $L_2$  norm,  $\mu, \nu$  and  $\theta$  being real numbers.

### 3.2. Regularized selection for proper, convex and lower-semicontinuous regularization criteria

Considering a regularization criterion  $\epsilon_2$  being a proper, convex and lower-semi-continuous (l.s.c) function, the regularized selection problem can be solved with the algorithm presented above. In this particular case,  $A$  is the identity matrix,  $F = \epsilon_2$  is the regularization criterion, and  $G = i_{\underline{\mathbf{X}}}$  is the convex indicator function that ensures that the solution  $\mathbf{X}$  is included into the convex set of admissible images  $\underline{\mathbf{X}}$ .  $i_{\underline{\mathbf{X}}}$  is defined by:

$$i_{\underline{\mathbf{X}}} : \mathbf{X} \mapsto i_{\underline{\mathbf{X}}}(\mathbf{X}) = \begin{cases} 0 & \text{if } \mathbf{X} \in \underline{\mathbf{X}} \\ +\infty & \text{if } \mathbf{X} \notin \underline{\mathbf{X}}, \end{cases} \quad (6)$$

$\underline{\mathbf{X}}$  is seen here as an optimization constraint. The general form of the regularized selection problem can be expressed as:

$$\min_{\mathbf{X} \in \Omega} \epsilon_2(\mathbf{X}) + i_{\underline{\mathbf{X}}}(\mathbf{X}). \quad (7)$$

A sufficient condition for the Chambolle-Pock algorithm to converge is  $\nu\mu\|A\|^2 < 1$ . In this case, setting  $\nu = 1$  and  $\mu = 1/2$  fulfills this condition as the linear operator  $A$  is the identity matrix. Note that  $\theta$  is set to 1, like in the third section of [11] and that it is possible to compute the proximal of the convex conjugate  $F^*$  of  $F$  with the relation  $\text{prox}_{F^*}(\mathbf{X}) = \mathbf{X} - \text{prox}_F(\mathbf{X})$  for  $\mathbf{X} \in \Omega$ .

Using these settings, the problem (7) can be solved by **Algorithm 1**.

---

**Algorithm 1** Chambolle-Pock iterative algorithm for regularized selection of interval-valued images

---

**Input:** Convex set of images  $\bar{\mathbf{X}}$ .

Initialization:

$v^{(0)} = \mathbf{0}$ ,  $\mathbf{X}^{(0)} = \mathbf{0}$ ,  $w^{(0)} = \mathbf{X}_{\text{center}}$  with  $\mathbf{0}$  being the null vector and  $\mathbf{X}_{\text{center}}$  the central image.

Step 1 -  $\epsilon_2$  minimization step:

$$v^{(k+1)} = v^{(k)} + w^{(k)} - \text{prox}_{\epsilon_2}(v^{(k)} + w^{(k)})$$

Step 2 - Projection on  $\bar{\mathbf{X}}$ :

$$\mathbf{X}^{(k+1)} = \text{prox}_{i_{\bar{\mathbf{X}}}}(\mathbf{X}^{(k)} + \mu v^{(k+1)})$$

Step 3 - Update:

$$w^{(k+1)} = 2\mathbf{X}^{(k+1)} - \mathbf{X}^{(k)}$$

---

**Output:** Regularized selection  $\mathbf{X}$ .

---

### 3.3. Regularized selection with $L_1$ and $L_2$ norm based criteria

In order to illustrate the performance of the proposed method, the regularized selection is presented in the context of SR reconstruction. We chose the widely used Total Variation (TV) [13] and the squared  $L_2$  norm of the image derivative as regularization criteria  $\epsilon_2$ . The latter are respectively denoted  $C_1$  and  $C_2$ . They are defined as:

$$\begin{aligned} C_1(\mathbf{X}) &= \sum_{\Omega} |\nabla(\mathbf{X})|_2, \\ C_2(\mathbf{X}) &= \sum_{\Omega} |\nabla(\mathbf{X})|_2^2, \end{aligned} \quad (8)$$

with  $\nabla$  being the discrete gradient approximation operator, and  $\Omega$  being the definition space of the image  $\mathbf{X}$ .

To use the algorithm presented above, we computed  $\text{prox}_{C_1}$  with the method described in [14] and  $\text{prox}_{C_2}$  with the conjugate gradient algorithm.

## 4. EXPERIMENTS

To compare the proposed  $C_1$  and  $C_2$  regularized selection methods, we used the well known  $L_1$  and  $L_2$  regularized IBP methods [15, 16]. We use the implementation provided in the

MDSP software<sup>1</sup>. The interval-based super-resolution method we use is presented in [8], where the central image is used to make the comparison with state of the art methods. The experiments presented in this section are made on both synthetic and natural images.

In both experiments, we consider only the case where movements between images are pure translations. In [8], the number of iterations of the reconstruction algorithm is set to 8. Here, this number is set to 20 to ensure that no implicit regularization is performed by early stop of the iterative process.

### 4.1. Experiment with synthetic images

In this experiment, we use an HR image of the Eia target. The Low Resolution (LR) image sequence is obtained by downscaling by a factor of 4 each HR corresponding image using an Epanechnikov interpolation kernel. Registration is achieved by considering the translation values used to mimic LR acquisitions. As the reference image is available, we selected the  $\beta$  parameter that provides the best PSNR with both IBP  $L_1$  and  $L_2$  reconstructions. Thus, we set  $\beta = 0.015$  for IBP  $L_1$  and  $\beta = 0.005$  for IBP  $L_2$ . For the regularized selection, the minimization of the regularization function was run until convergence for both  $C_1$  and  $C_2$  selections.

SR method	Iterative back-projection			
	Precise		Imprecise	
Regularization cost function	$L_1$	$L_2$	$C_1$	$C_2$
PSNR	19.635	17.935	20.653	19.097

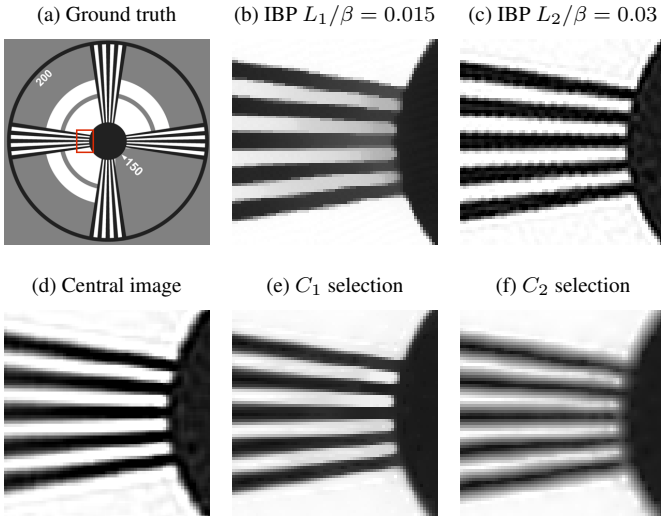
**Table 1:** Quantitative assessment of the proposed method

Table 1 shows that the regularized selection leads to a higher PSNR value in both  $C_1$  and  $C_2$  cases.  $C_1$  and  $C_2$  selection are closer, in PSNR, to the original image, than their respective competitors IBP  $L_1$  and IBP  $L_2$ .

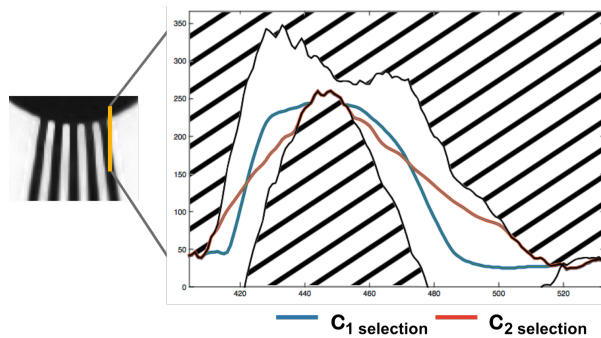
In Fig. 1 (a-f), we can observe that only IBP  $L_2$  remains with Gibbs effects. Even if these artifacts disappear with the  $C_2$  selection, the quadratic nature of the regularization term leads to a blurred image. The results are more significant with  $L_1$  regularization terms. The best IBP  $L_1$  is close to the  $C_1$  selection, but we can notice that  $C_1$  selection leads to a better separation between the white and black strips.

Fig. 2 illustrates the behavior of the regularized selections that satisfy both data-fitting (interval constraints) and regularization term. We can see that the properties of the regularization terms are respected. The  $C_1$  selection separates the strips with a step profile, while  $C_2$  selection tends to smooth the image.

<sup>1</sup><https://users.soe.ucsc.edu/~milanfar/SR-Software.html>



**Fig. 1:** HR reconstructions of Eia target with different methods.



**Fig. 2:**  $C_1$  and  $C_2$  regularized selection profiles

#### 4.2. Independence of the method w.r.t. the data

The following qualitative experiment is based on 9 shifted natural acquisitions of a book cover. It aims at showing the independence of our regularization method with respect to the content of the image (we focus on  $L_1$  regularization criterion here).

To reconstruct the IBP  $L_1$  HR image of the book cover presented in Fig. 3, we select  $\beta_1 = 0.005$  and  $\beta_2 = 0.013$  that respectively give the better trade-off between edges preservation and smoothing in the right and left zoomed image patches. We can see in Fig. 3 (a) that the reconstruction with  $\beta_1$  that gives satisfying detail preservation in the right patch, gives poor results (Gibbs artifacts) in the left patch. Conversely, as presented in Fig. 3 (c), the reconstruction with  $\beta_2$  that gives better results for the left patch, results in an important loss of the flower details in the right patch. This experiment highlights the image content dependence of the  $\beta$  choice. As opposed to the  $\beta$  dependent regularized reconstructions, we can observe in Fig. 3 (b) that the  $C_1$  selection has an interesting balance

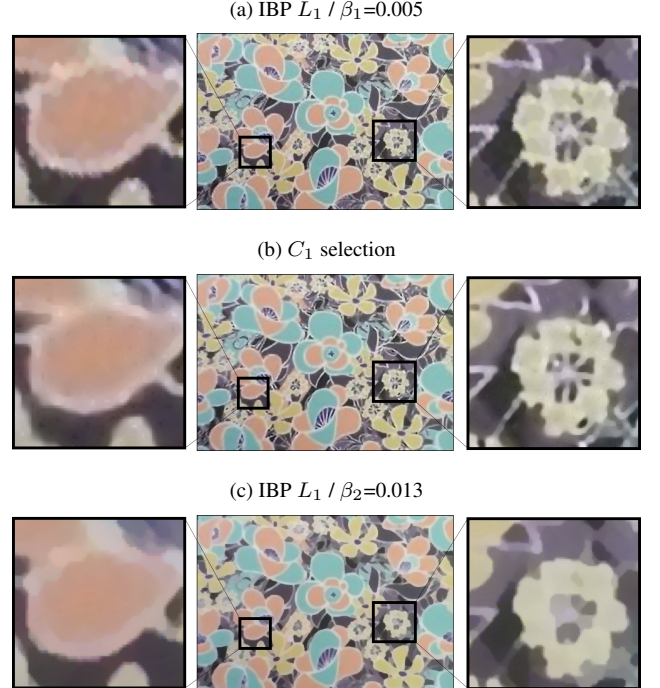


**Fig. 3:** Comparison of IBP  $L_1$  and  $C_1$  selection on a book cover

between preserving the edges and smoothing the more homogeneous parts of the image. Indeed, the right and left patches obtained with regularized selection are at least as satisfactory as the best IBP  $L_1$  right and left patches. Notice that another advantage of this method is that, as the reconstruction process is independent of the regularization, it can be performed as a post-processing. If the user is not satisfied by the result, it would then be both easy and fast to perform regularized selections with other regularization criteria.

## 5. CONCLUSION

In this paper, we presented a new method of regularization, that we called regularized selection. This method applies to interval based signals. We illustrated the behavior of the method on super-resolution reconstruction examples. Using the interval-based algorithm presented in [8], we showed that the presented method is easy to use, and leads to more homogeneous and robust results than its state-of-the-art competitors. This method has the advantage not to require any regularization parameter. The fact that the regularized selection is *a posteriori* allows to run different regularized selections in the set of admissible solutions in a reduced amount of time, while usual regularized methods require the algorithm to restart from scratch with every new type or weight of regularization. In further works, we will try to find and adapt other regularization criteria to other applications.

## 6. REFERENCES

- [1] M.E. Kilmer and D.P. OLeary, “Choosing regularization parameters in iterative methods for ill-posed problems,” *SIAM J. Matrix Anal. and Appl.*, vol. 22, no. 4, pp. 1204–1221, 2001.
- [2] A. Nemirovskii, “The regularization properties of adjoint gradient method in ill-posed problems,” *USSR Computational Mathematics and Mathematical Physics*, vol. 26, no. 2, pp. 7–16, 1986.
- [3] H.E. Flemming, “Equivalence of regularization and truncated iteration in the solution of ill-posed image reconstruction problems,” *Linear Algebra Appl.*, vol. 130, pp. 133–150, 1990.
- [4] O. Strauss, A. Lahrech, A. Rico, D. Mariano-Goulart, and B. Telle, “NIBART: A new interval based algebraic reconstruction technique for error quantification of emission tomography images,” in *International Conference on Medical Image Computing and Computer-Assisted Intervention*. Springer Berlin Heidelberg, 2009, pp. 148–155.
- [5] F. Graba and O. Strauss, “An interval-valued inversion of the non-additive interval-valued f-transform: Use for upsampling a signal,” *Fuzzy Sets and Systems*, vol. 288, pp. 26–45, 2016.
- [6] S. Destercke and O. Strauss, “Filtering with clouds,” *Soft Computing*, vol. 16, no. 5, pp. 821–831, 2012.
- [7] F. Graba, K. Loquin, F. Comby, and O. Strauss, “Guaranteed reconstruction for image super-resolution,” in *Fuzzy Systems (FUZZ), 2013 IEEE International Conference on*. IEEE, 2013, pp. 1–8.
- [8] F. Graba, F. Comby, and O. Strauss, “Non-additive imprecise image super-resolution in a semi-blind context,” *IEEE Transactions on Image Processing*, 2017, to appear.
- [9] Kevin Loquin and Olivier Strauss, “On the granularity of summative kernels,” *Fuzzy sets and systems*, vol. 159, no. 15, pp. 1952–1972, 2008.
- [10] O. Strauss and A. Rico, “Towards interval-based non-additive deconvolution in signal processing,” *Soft computing*, vol. 16, no. 5, pp. 809–820, 2012.
- [11] Antonin Chambolle and Thomas Pock, “A first-order primal-dual algorithm for convex problems with applications to imaging,” *Journal of Mathematical Imaging and Vision*, vol. 40, pp. 120–145, 2010.
- [12] P.L. Combettes and J.C. Pesquet, “Proximal splitting methods in signal processing,” *Fixed-Point for Inverse Problems in Science and Engineering*, pp. 185–212, 2011.
- [13] L. Rudin, S. Osher, and E. Fatemi, “Nonlinear total variation based noise removal algorithms,” *Physica D*, vol. 60, pp. 259–268, 1992.
- [14] Laurent Jacques, Davis Hammond, and Jalal M. Fadili, “Dequantizing compressed sensing: When oversampling and non-gaussian constraints combine,” *IEEE Transactions on Information Theory*, vol. 1, no. 57, pp. 559–571, 2011.
- [15] M. Irani and S. Peleg, “Improving resolution by image registration,” *CVGIP: Graphical Models and Image Proc.*, vol. 53, pp. 231–239, 1991.
- [16] A. Zomet and S. Peleg, “Efficient super-resolution and applications to mosaics,” *ICPR*, vol. 1, no. 579–583, 2000.